ELSEVIER

PII: S0032-3861(98)00115-3

Polymer Vol. 39 No. 18, pp. 4369–4378, 1998

0032-3861/98/$19.00+0.00

High temperature properties of poly(styrene-co-alkylmaleimide) foams prepared by high internal phase emulsion polymerization

Joseph R. Duke Jr.[a,*], Mark A. Hoisington[b], David A. Langlois[a] and Brian C. Benicewicz[c]

[a]*Los Alamos National Laboratory, Materials Science and Technology Division, Polymers and Coatings Group, MS E549, Los Alamos, NM 87545, USA*

[b]*3M Austin Center, Building A145-4S-02, 6801 River Place Blvd., Austin, TX 78726-9000, USA*

[c]*Department of Chemistry, Cogswell Building, Rensselaer Polytechnic Institute, Troy, NY 12180, USA*

(Received 30 September 1997; revised 30 January 1998; accepted 2 February 1998)

The influence of three N-substituted maleimides on the processing, thermal, and mechanical performance of high internal phase emulsion (HIPE) polymerized foams are investigated. N-propylmaleimide, N-butylmaleimide, and N-cyclohexylmaleimide were copolymerized with styrene and crosslinked with either divinylbenzene or bis(3-ethyl-5-methyl-4-maleimide-phenyl)methane in a HIPE polymerization process. The foam samples were evaluated by dynamic mechanical analysis, thermogravimetric analysis, compression strength measurements, and scanning electron microscopy. All maleimide modifiers produced increases in the foam glass transition temperature (T_g) as a function of the maleimide concentration. However, the degree of T_g improvement was strongly dependent on the N-substituted maleimide used during processing. Cyclohexylmaleimide produced higher T_g foams than propylmaleimide, which produced higher T_g foams than butylmaleimide. In addition, the N-substituted maleimide solubility in both the oil and water phases played important roles in the processing and final open-celled microstructure. The preferred N-substituted maleimide modifier should possess high solubility in the oil phase and insolubility in the water phase.

(Keywords: foams; high internal phase emulsion; styrene)

INTRODUCTION

High internal phase emulsion (HIPE) polymerizations were first used to produce isotropic, open celled, polymeric foams in 1982 [1]. This process forms foams from a water-in-oil HIPE in which the oil phase is composed of monomers such as styrene or acrylates mixed with small concentrations of crosslinking agents. For emulsions to be classified as a HIPE, the internal or discontinuous phase must represent at least 76% of the emulsion by volume. This minimum volume is the theoretical volume that close packed spheres occupy in a given volume. After obtaining a HIPE, the foam is produced by heating the system to initiate polymerization of the monomers and then drying the cured open-celled polymeric material to remove the water.

These HIPE polymeric foams are of interest because of their low density, open celled morphology, structural properties, and high absorbency capabilities. A number of patents have been issued covering applications from absorbents for body fluids to ion exchange systems[2–27]. Los Alamos National Laboratory has developed an expertise in the HIPE polymerized foam systems for applications in inertial confinement fusion experiments, as well as, applications involving nuclear ion separations[11–37]. Our recent effort with HIPE foams attempt to combine their low density and structural property characteristics with improved thermal performance to produce high temperature, structural, polymeric foam systems[38].

Heat resistant, structural foams have potential uses in a wide range of applications including core material for composite sandwich panels, filler for the cells of honeycomb core, and as acoustic or thermal insulation in elevated temperature environments such as engine compartments and enclosures. Development of high temperature HIPE foams could provide significant advantages over commercial blown and extruded foam systems. HIPE foams can be processed over a wide range of densities (20–320 mg/cm^3), the emulsion produced during processing allows for near-net-shape casting capabilities, and the final foam possesses isotropic properties. Blown and extruded foam systems cannot provide the HIPE processing capabilities with isotropic properties.

Our approach to improve the glass transition temperature (T_g) of the HIPE foams has been to copolymerize styrene with N-substituted maleimide and bismaleimide (BMI) monomers [38]. Copolymerization of styrene with N-substituted maleimides has been widely used in the past to produce heat resistant thermoplastic materials[39–45]. However, there are many difficulties in attempting the maleimide–styrene copolymerization in a HIPE such as lower polymerization temperatures, limited maleimide

* To whom correspondence should be addressed

solubility in styrene, and difficulty obtaining a stable HIPE with a styrene/maleimide oil. Initially we used N-ethylmaleimide and bis(3-ethyl-5-methyl-4-maleimide-phenyl)-methane (BMI-70) to copolymerize with styrene in the HIPE polymerization process[38]. This work demonstrated that styrene–maleimide copolymer foams could be obtained in a HIPE polymerization process to produce high T_g, structural, polymeric foams.

Although our initial efforts were successful, the choice of N-ethylmaleimide presented some problems. N-ethylmaleimide was chosen for our initial studies because it was highly soluble in styrene, approximately 60% by weight. However, N-ethylmaleimide is also partially soluble in water, approximately 5% by weight. In the HIPE polymerization process, oil phase components need to be essentially insoluble in the water phase to provide a distinct boundary between the phases and produce uniform open cellular structures. Partially water soluble monomers increase the difficulty in obtaining stable HIPE's. N-ethylmaleimide was able to produce improvements in the polymeric foam T_g, but the maximum concentration of N-ethylmaleimide was limited to less than 50% by weight. When the concentration of N-ethylmaleimide, or the combination concentration of N-ethylmaleimide with BMI-70 reached 50% by weight, a stable HIPE could no longer be obtained. We attributed this maximum in N-ethylmaleimide concentration partly to the 5% solubility in water.

Our most recent work has attempted to improve upon the high temperature foam systems by using three other N-substituted maleimides with lower water solubility than N-ethylmaleimide; N-propylmaleimide, N-butylmaleimide, and N-cyclohexylmaleimide. In this work, we have investigated the solubility and steric effects of the N-substituted maleimides on the thermal, processing, and mechanical performance of the HIPE copolymerized foams.

EXPERIMENTAL

Materials

N-cyclohexylmaleimide was obtained from the Ken Seika Corporation. Bis(3-ethyl-5-methyl-4-maleimide-phenyl)methane was obtained from Ihara Chemical, with the help of Ken Seika Corp., under the product name BMI-70. N-propylmaleimide and N-butylmaleimide were both synthesized in our laboratory from the reaction between maleic anhydride and N-propylamine and N-butylamine respectively, according to the general method of Mehta *et al.*[46] Stabilized styrene (STY) was used as received from VWR Scientific, and a 55–60% active divinylbenzene (DVB) containing ethyl vinyl benzene, naphthalene, and diethyl benzene was used as received from Polysciences Incorp. Potassium persulfate was obtained from Aldrich Chemical Corp. and used as the free radical polymerization initiator. Sorbitan Monooleate (SMO) was used as the emulsifying agent and was obtained from the Henkel Corp. as Emsorb 2500. The chemical structures of the monomeric oil phase components are shown in *Figure 1*.

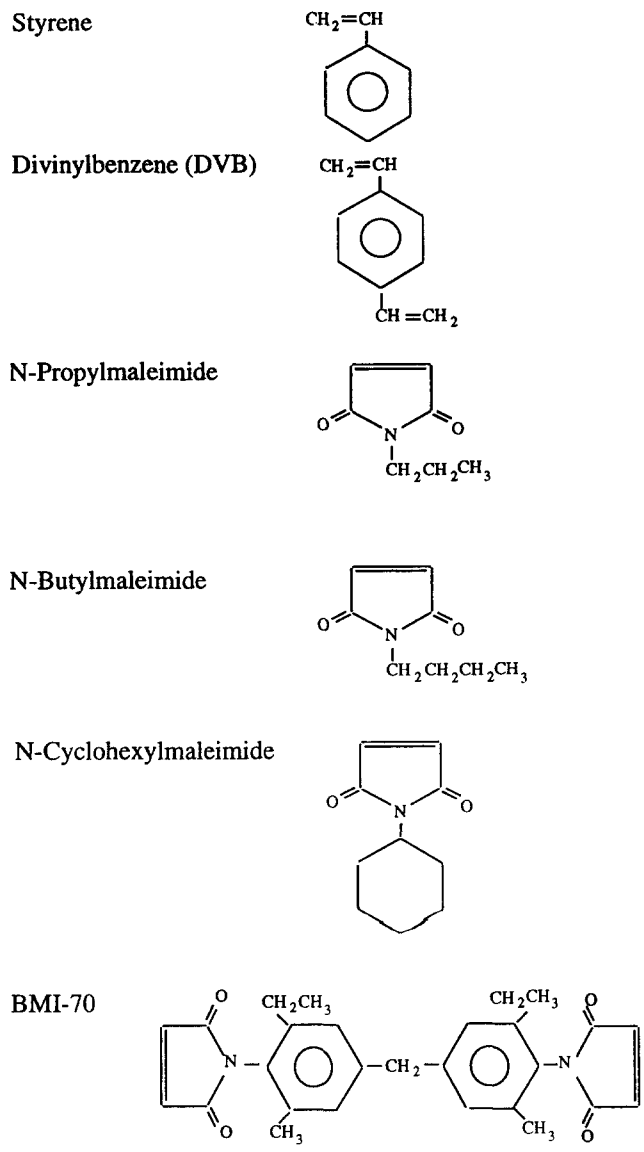

Figure 1 Chemical structure of oil phase monomeric components

Processing

The foams were processed by first dissolving the maleimide and BMI-70 into the STY/DVB monomers; the SMO was then added to the monomer mixture. In all foams processed, a total oil weight of 7.5 g was prepared and placed in a 100-ml Qorpak jar. The oil phase was then mechanically stirred at ≈ 600–800 rpm while 92.5 g of distilled water containing 1.5 g/l potassium persulfate was added dropwise. After all the water had been added, the emulsion was further stirred for 5 min at a speed of ≈ 900 rpm and for 5 min at a speed of 1000 rpm. The jars were capped and put in a convection oven at 60°C to cure overnight.

After polymerization, the foams were removed from the Qorpak jars and returned to the convection oven to dry at 60°C. Drying times varied from several hours to 48 h depending on the morphology of the cells. The dried foams were then postcured at 250°C under vacuum overnight.

Compositions of the oil phase used in processing foam samples will be presented using weight percentages. The SMO concentrations will be reported as percentage by weight of the entire oil phase. Monomer concentrations will be reported as percentage by weight of only the total monomer weight in the oil phase. For example, a 100-g sample of oil containing 15% SMO, 10% DVB, and 90% styrene would contain 15 g SMO, 8.5 g DVB, and 76.5 g styrene. This convention is used because the SMO does not take part in the polymerization reaction and the majority of the SMO volatalizes and is removed during postcure.

Analysis

Dynamic mechanical analysis (DMA) was done with a Rheometrics RDA II mechanical spectrometer. The T_g of the foam samples was defined as the peak in the tan delta curve. A clamping fixture capable of gripping onto the foam samples was machined to fit into the normal Rheometrics adapters. Testing was done at a fixed frequency of 1 Hz, and the temperature was stepped at 5°C increments from 30°C to a maximum temperature of 350°C in a nitrogen environment.

Thermogravimetric Analysis (TGA) was done with a Polymer Laboratory TGA Model 1500 to examine thermal stability behaviour. Foam samples were dynamically run at 10°C/min from 10 to 500°C in both air and nitrogen environments.

Foam compression strengths were evaluated on an Instron Model 4483 testing frame. One sample of each composition was tested to quickly screen mechanical performance. Samples were cylindrical in shape $\approx$ 25 mm (1.0 in.) high and 45 mm (1.77 in.) in diameter and tested at a rate of 0.25 mm/min (0.1 in./min).

Morphologies of the foam samples were evaluated by scanning electron microscopy (SEM), using a Hitachi S520 microscope after mounting the samples on stalks, cutting them with a Vibratome razor, and then coating them with a paladium gold mixture.

EXPERIMENTAL RESULTS

A series of styrene based foam samples crosslinked with divinylbenzene (DVB) or BMI-70 was processed with each of the N-substituted maleimide modifiers: N-propylmaleimide, N-butylmaleimide, and N-cyclohexylmaleimide. Each series examined the effects of increasing maleimide concentration on the processing, microstructure, thermal, and mechanical performance in comparison to a standard foam system containing 90% styrene and 10% DVB. Specific sample identifications and compositions are given in *Table 1*, *Table 2* and *Table 3* for the maleimide modified foams.

Processing

Processing of HIPE polymerized foams can be qualitatively evaluated by characterizing the emulsion obtained during mixing, and the final foam produced. The emulsion obtained during mixing should be smooth and free of water separation, while the final foam should conform to the container and have a uniformly smooth surface. In our previous work with N-ethylmaleimide, a processing limitation of 50% N-ethylmaleimide by weight or combined concentration of 50% N-ethylmaleimide and BMI-70 by weight was determined [36]. When the maleimide concentration reached 50% by weight, a HIPE could not be obtained, and disconnected polymer particles were produced during the polymerization. In part, we attributed this concentration limitation to the solubility of N-ethylmaleimide in water, $\approx$ 5% by weight.

Accordingly, N-propylmaleimide and N-butylmaleimide were used in this study because of their higher solubility in

Table 1 Sample identifications and compositions of N-propylmaleimide modified foams

	Percentage by weight of each component			
Sample	Styrene	DVB	N-propylmaleimide	BMI-70
ProMI-1	90	10	0	0
ProMI-2	80	10	10	0
ProMI-3	70	10	20	0
ProMI-4	60	10	30	0
ProMI-5	50	10	40	0
ProMI-6	40	10	50	0
ProMI-7	70	0	10	20
ProMI-8	60	0	20	20
ProMI-9	55	0	25	20
ProMI-10	50	0	30	20

Table 2 Sample identifications and compositions of N-butylmaleimide modified foams

	Percentage by weight of each component			
Sample	Styrene	DVB	N-butylmaleimide	BMI-70
ButMI-1	90	10	0	0
ButMI-2	80	10	10	0
ButMI-3	70	10	20	0
ButMI-4	60	10	30	0
ButMI-5	50	10	40	0
ButMI-6	40	10	50	0
ButMI-7	70	0	10	20
ButMI-8	60	0	20	20
ButMI-9	55	0	25	20
ButMI-10	50	0	30	20
ButMI-11	45	0	35	20

Table 3 Sample identifications and compositions of N-cyclohexylmaleimide modified foams

	Percentage by weight of each component			
Sample	Styrene	DVB	N-cyclohexylmaleimide	BMI-70
CyMI-1	90	10	0	0
CyMI-2	80	10	10	0
CyMI-3	70	10	20	0
CyMI-4	60	10	30	0
CyMI-5	50	10	40	0
CyMI-6	40	10	50	0
CyMI-7	70	0	10	20
CyMI-8	60	0	20	20
CyMI-9	55	0	25	20
CyMI-10	50	0	30	20

styrene and lower solubility in water compared to N-ethylmaleimide. The increasing alkyl chain length of the N-substitution increases the hydrophobicity of the monomer leading to an increase in styrene solubility and a decrease in the water solubility. N-ethylmaleimide was $\approx$ 60% by weight soluble in styrene and 5% by weight soluble in water. N-propylmaleimide was $\approx$ 89% by weight soluble in styrene and less than 2% by weight soluble in water; N-butylmaleimide was greater than 90% by weight soluble in styrene and less than 1% by weight soluble in water. This increased styrene solubility and lower water solubility increased the maximum concentration of maleimide modifier that could be successfully used in the HIPE process.

For the DVB crosslinked systems, Samples ProMI-1 to ProMI-5 (*Table 1*) and Samples ButMI-1 to ButMI-5 (*Table 2*) produced smooth emulsions during processing and high quality final foams. When the maleimide concentration reached 50% by weight, Samples ProMI-6 and ButMI-6 also produced a smooth HIPE. However, Sample ProMI-6 produced a fragile final foam that contained large pot marks throughout caused by water separation during polymerization, and Sample ButMI-6 exhibited some shrinkage during drying. In the BMI-70 crosslinked systems, all N-propylmaleimide and N-butylmaleimide samples were able to produce high quality foams including ProMI-10 and ButMI-10, which contained a total maleimide modifier concentration of 50% by weight, and ButMI-11, which contained a total maleimide modifier concentration of 55% by weight.

In addition to increasing the maleimide concentration capabilities in a HIPE process, the increased styrene solubility of N-propylmaleimide and N-butylmaleimide decreased the HIPE viscosity. In our previous work with N-ethylmaleimide, an increasing emulsion viscosity trend was observed with increasing maleimide concentration. This increase in viscosity was especially evident in the BMI-70 crosslinked systems. To take advantage of the near-net-shape processing capabilities of the HIPE foam process, the emulsion must freely conform to the shape of the mold used during processing. At high concentrations of N-ethylmaleimide, the emulsion viscosity increased sufficiently to make mold conformation difficult. Thus, the lower viscosity of the N-propylmaleimide and N-butylmaleimide systems also represents a significant processing benefit.

N-cyclohexylmaleimide was chosen for these experiments to investigate the effects of a bulky N-substitution on the maleimide ring as well as the use of an essentially water insoluble maleimide monomer. The trade-off with using N-cyclohexylmaleimide is a lower styrene solubility, only about 33% by weight. For the DVB crosslinked systems, Samples CyMI-1 to CyMI-6 (*Table 3*), all produced smooth emulsions and good quality final foams. However, when the concentrations of N-cyclohexylmaleimide exceeded the solubility limit of 33% by weight (Samples CyMI-5 and CyMI-6), solid polymer particles were visibly embedded throughout the foam under examination with SEMs. These polymer particles appeared to be undissolved N-cyclohexylmaleimide. For the BMI-70 crosslinked samples, Samples CyMI-7 to CyMI-10 all produced a HIPE during mixing and high quality final foams except for a small amount of solid polymer particles observed throughout foam Sample CyMI-10. These solid polymer particles observed throughout the foams stress the importance of using styrene soluble maleimide modifiers.

Although all N-cyclohexylmaleimide modified samples were able to produce foams, the emulsion viscosity produced during mixing was significantly higher than all other maleimide systems we have investigated. The DVB crosslinked systems showed only a small increasing trend in viscosity with increasing N-cyclohexylmaleimide concentration, but the BMI-70 crosslinked samples exhibited large increases in emulsion viscosity with increasing N-cyclohexylmaleimide concentration. This increase in emulsion viscosity appears to be a consequence of the lower styrene solubility of the N-cyclohexylmaleimide. These viscosity observations demonstrate an additional reason for using maleimide monomers with high styrene solubility.

Morphology

SEM photomicrographs were taken of each of the foam samples to examine the microstructure obtained after processing. *Figure 2* shows representative SEM photomicrographs for foams containing N-propylmaleimide, N-butylmaleimide, and N-cyclohexylmaleimide. The typical HIPE foam morphology before maleimide modification is shown in *Figure 2a*. A cell size of $\approx$ 10 mm is generally obtained with interconnecting pores of $\approx$ 1–3 mm. Each maleimide modified system produced different influences on the foam morphology.

When N-propylmaleimide was used to modify the foam systems, the basic open celled structure was maintained up to a concentration of 40% N-propylmaleimide by weight. As the N-propylmaleimide concentration was increased, there was an increase in size of the interconnecting pores, a decrease in cell size, and some signs of break-up in the cell structure (*Figure 2b*). The cells contained less of a wall and more of a strut configuration. As the N-propylmaleimide concentration reached 50% by weight, the open cell

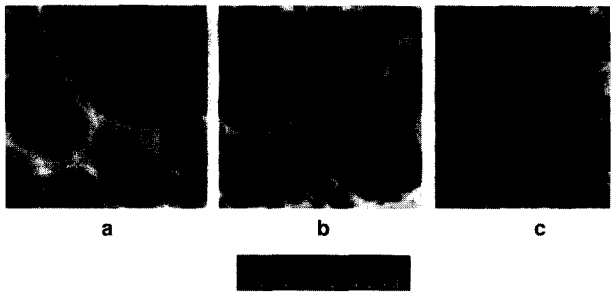

Figure 2 Scanning electron photomicrographs of representative foams: (a) a styrene–divinylbenzene foam; (b) an alkylmaleimide modified foam; (c) an alkylmaleimide foam that has separated into particles

structure was no longer visible. The foam morphology was composed of connected polymer particles which produced an extremely fragile foam (*Figure 2c*).

DVB crosslinked N-butylmaleimide modified foams performed slightly better than the N-propylmaleimide systems. As the N-butylmaleimide concentration was increased, a similar strut configuration was observed with some break-up in the cellular structure. However, the cellular structure remained intact to higher concentrations with N-butylmaleimide than with N-propylmaleimide.

DVB crosslinked N-cyclohexylmaleimide modified foams performed significantly better than the other maleimide systems. All concentrations of N-cyclohexylmaleimide produced an open cell morphology typical of HIPE foams with only a slight amount of break-up in the cell structure. There does appear to be a small decrease in cell size and more of a strut configuration with the addition of N-cyclohexylmaleimide, but the basic open celled HIPE morphology was created at all concentrations.

Similar trends were observed in the BMI-70 crosslinked foam samples. Initially, at low maleimide modifier concentrations, all systems show some signs of cellular break-up due to the 20% BMI-70 used as the crosslinking agent. As the maleimide modifier concentrations increased, the N-propylmaleimide modified foams produced the largest amount of break-up in the cellular structure. N-butylmaleimide modified foams retained the open cell structure for all samples with only a small amount of cellular break-up, while the N-cyclohexylmaleimide modified foams produced the most consistent open cell structure over the entire composition range.

The importance of using a water insoluble maleimide was apparent when the SEMs of the three maleimide modified systems were compared. As the water solubility of the maleimide modifiers was decreased, there was a corresponding increase in the quality of cellular structure formed. Although the solubility limit of N-cyclohexylmaleimide in styrene was reached during processing, there was no detrimental effect on the cell structure. The insoluble N-cyclohexylmaleimide was incorporated into the foam as solid polymer particles. Therefore, the optimum maleimide modifier for a styrene based HIPE foam process would possess a high solubility in styrene and insolubility in water.

Dynamic mechanical analysis

The glass transition temperature (T_g) of each of the foam samples was defined as the peak in tan delta obtained from DMA. All foam samples produced similar T_g trends to our previous work with N-ethylmaleimide modified foams. In the DVB crosslinked N-ethylmaleimide foams, the T_g increased linearly with maleimide modifier concentration. For every 10% increase in N-ethylmaleimide concentration there was an increase of $\approx$ 20°C in the measured foam T_g. A maximum T_g of 204°C was obtained for a foam containing 40% N-ethylmaleimide by weight. For the BMI-70 crosslinked N-ethylmaleimide foams, the T_g was essentially independent of N-ethylmaleimide concentration at 219°C. Increases in N-ethylmaleimide concentration produced a narrower transition region, but the peak temperature of the tan delta peak was unaffected. Although the N-propylmaleimide, N-butylmaleimide, and N-cyclohexylmaleimide foams exhibited similar trends to N-ethylmaleimide foams, the amount of T_g improvement was strongly dependent on the choice of maleimide modifier used in processing.

In the DVB crosslinked N-propylmaleimide foams, the T_g of foam Samples ProMI-1 to ProMI-6 (*Table 1*) increased with N-propylmaleimide concentration. *Figure 3* shows that with every 10% increase in N-propylmaleimide concentration, the foam T_g increased $\approx$ 10°C. A maximum T_g was determined to be $\approx$ 194°C when 50% N-propylmaleimide by weight was used during processing. In comparison to our results with N-ethylmaleimide, the increase in T_g with N-propylmaleimide was significantly less than the 20°C provided by adding 10% N-ethylmaleimide. The increasing chain length of the maleimide N-substitution decreased the corresponding T_g of the foam system. This T_g trend was also seen in the DVB crosslinked N-butylmaleimide foam system. Although *Figure 4* shows the foam T_g increasing with increasing N-butylmaleimide concentration, Samples ButMI-1 to ButMI-6 (*Table 2*) exhibited a T_g increase of only 5–10°C with every 10% addition of N-butylmaleimide. Therefore, a significant sacrifice in T_g is produced with increasing N-substitution chain length.

When the linear N-alkyl maleimide was changed to a bulky group with the use of N-cyclohexylmaleimide, the same correlation between T_g and maleimide concentration was obtained. However, larger T_g improvements were observed with the use of N-cyclohexylmaleimide. *Figure 5* shows that the DVB crosslinked N-cyclohexylmaleimide foams produced approximately a 15°C improvement with every 10% addition of N-cyclohexylmaleimide. A

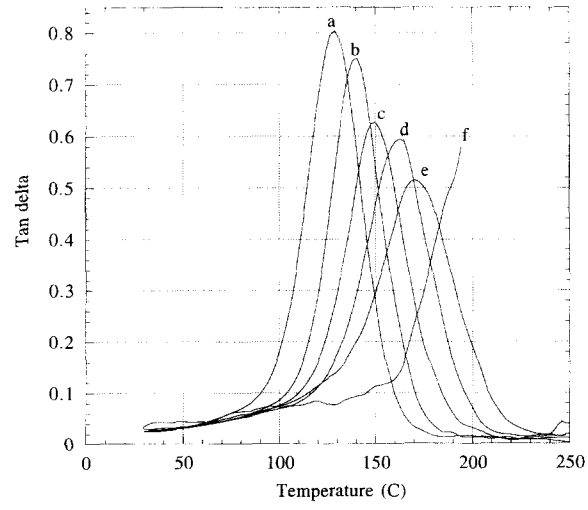

Figure 3 DMA curves as a function of temperature for N-propylmaleimide modified foams crosslinked with DVB: (a) Sample ProMI-1, peak at 129°C; (b) Sample ProMI-2, peak at 139°C; (c) Sample ProMI-3, peak at 149°C; (d) Sample ProMI-4, peak at 164°C; (e) Sample ProMI-5, peak at 169°C; (f) ProMI-6, peak at > 194°C.

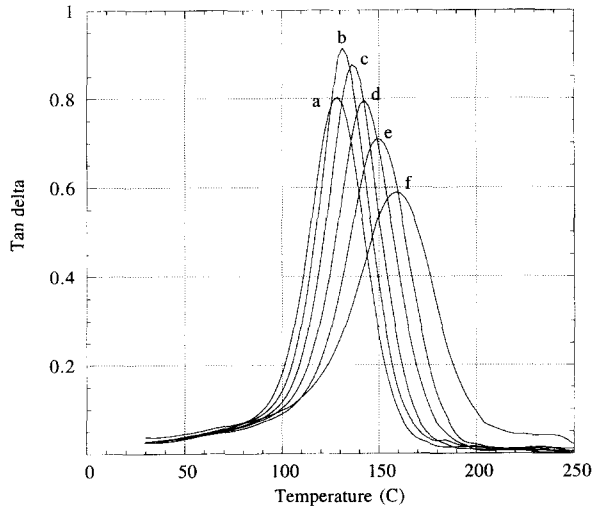

Figure 4 DMA curves as a function of temperature for N-butylmaleimide modified foams crosslinked with DVB: (a) Sample ButMI-1, peak at 129°C; (b) Sample ButMI-2, peak at 130°C; (c) Sample ButMI-3, peak at 134°C; (d) Sample ButMI-4, peak at 144°C; (e) Sample ButMI-5, peak at 149°C; (f) ButMI-6, peak at 159°C

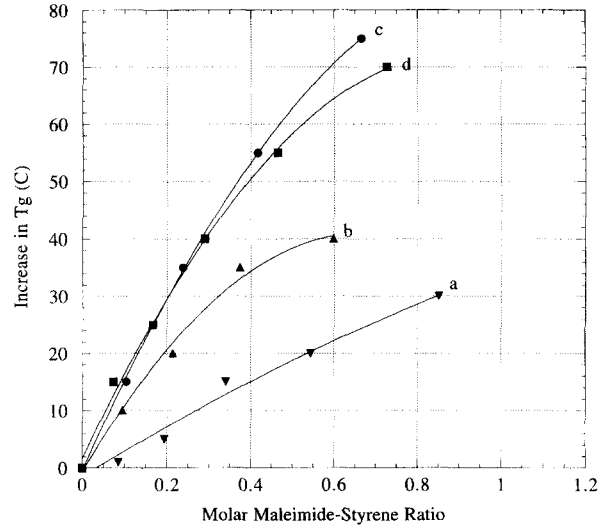

Figure 6 Increase in T_g of high temperature foams crosslinked with DVB in comparison to 90% styrene/10% DVB foam as a function of the molar ratio of maleimide to styrene used in processing: (a) N-butylmaleimide modified foams; (b) N-propylmaleimide modified foams; (c) N-ethylmaleimide modified foams; (d) N-cyclohexylmaleimide modified foams

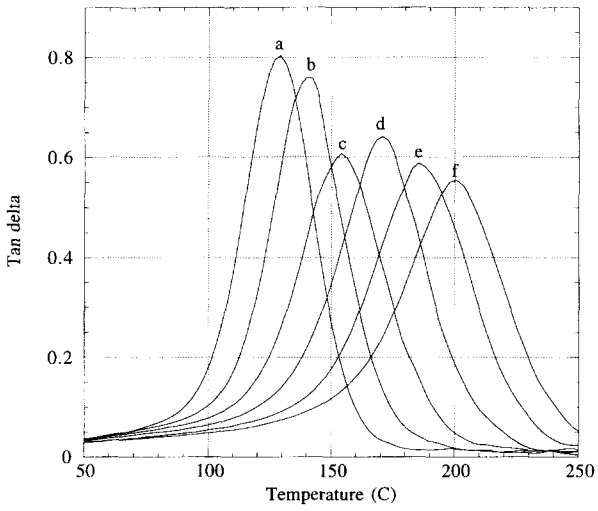

Figure 5 DMA curves as a function of temperature for N-cyclohexylmaleimide modified foams crosslinked with DVB: (a) Sample CyMI-1, peak at 129°C; (b) Sample CyMI-2, peak at 144°C; (c) Sample CyMI-3, peak at 154°C; (d) Sample CyMI-4, peak at 169°C; (e) Sample CyMI-5, peak at 184°C; (f) CyMI-6, peak at 199°C

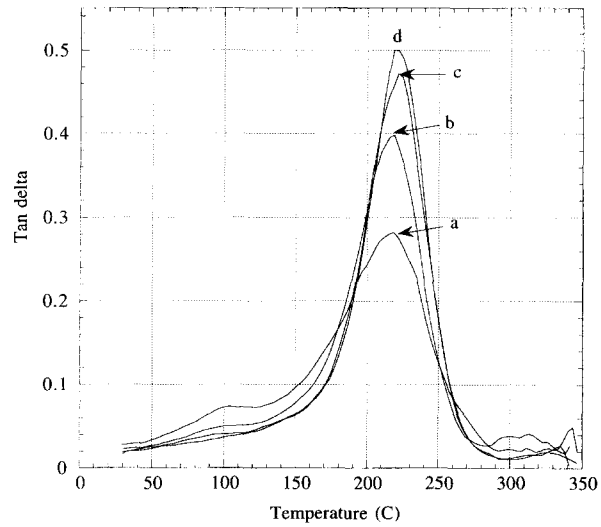

Figure 7 DMA curves as a function of temperature for N-cyclohexylmaleimide modified foams crosslinked with BMI-70: (a) Sample CyMI-7; (b) Sample CyMI-8; (c) Sample CyMI-9; (d) Sample CyMI-10. All tan delta peaks occur at ≈ 218°C

maximum T_g of 199°C was obtained with the incorporation of 50% N-cyclohexylmaleimide by weight. Although this T_g improvement is lower than the N-ethylmaleimide modified foams, this analysis has not taken the maleimide formula weight differences into account.

Concentrations of the maleimide modifiers in these foam systems have been expressed in percentage by weight. When we correct for the increasing formula weights of the maleimide modifiers, T_g improvements can be compared on a molar basis. *Figure 6* plots the increase in T_g of a standard foam system containing 90% styrene and 10% DVB as a function of the molar ratio of maleimide modifier to styrene used in processing. This figure illustrates the large decrease in T_g improvement with increasing N-substitution chain length. Although this decreasing trend in T_g should be expected, the significant amount of decrease was unexpected. In addition, *Figure 6* illustrates that N-cyclohexylmaleimide and N-ethylmaleimide provide approximately the same T_g increase when compared on a molar basis. Therefore, the maximum foam thermal performance is obtained by using a maleimide with a bulky or short chain N-alkyl substitution.

In the BMI-70 crosslinked foam samples, the T_g was essentially independent of maleimide concentration, but the degree of T_g improvement was dependent on the maleimide chosen for processing. N-cyclohexylmaleimide produced a foam with the highest T_g. *Figure 7* shows the DMA results for the BMI-70 crosslinked N-cyclohexylmaleimide foams. All samples show a peak in the DMA curves near 218°C; however, with increasing N-cyclohexylmaleimide concentration the transition region narrows. The peak in the DMA curve is controlled by the BMI-70 crosslinks, and the addition of N-cyclohexylmaleimide increases the thermal stability of copolymer blocks between crosslinks. BMI-70 crosslinked N-ethylmaleimide foams showed the same

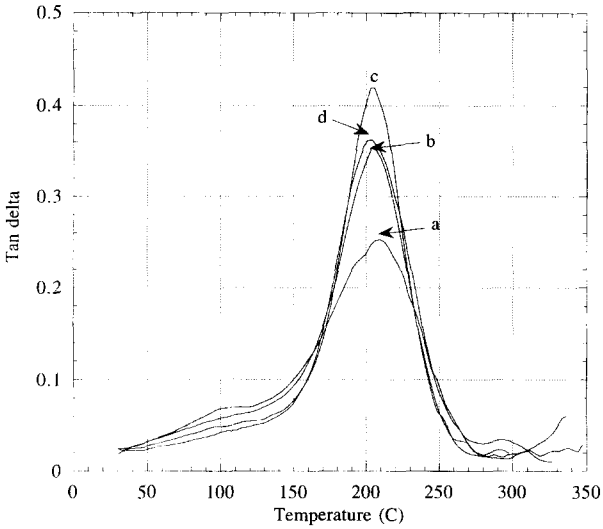

Figure 8 DMA curves as a function of temperature for N-propylmaleimide modified foams crosslinked with BMI-70: (a) Sample ProMI-7; (b) Sample ProMI-8; (c) Sample ProMI-9; (d) Sample ProMI-10. All tan delta peaks occur at ≈ 204°C

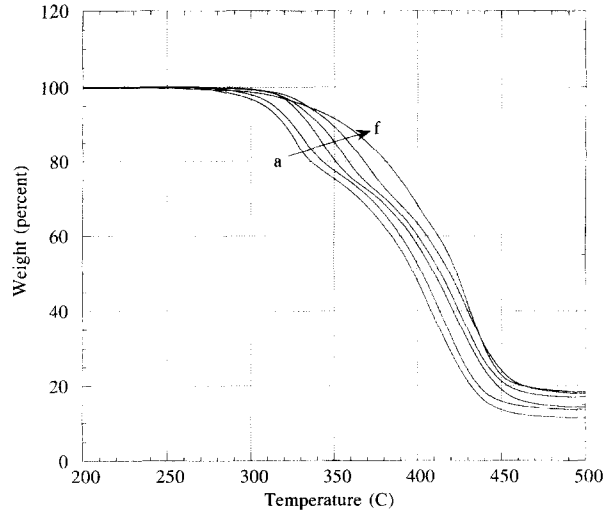

Figure 10 Thermogravimetric analysis in air of N-propylmaleimide modified foams crosslinked with DVB showing increasing thermal stability with increasing propylmaleimide concentration from (a) Sample ProMI-1 to (f) Sample ProMI-6

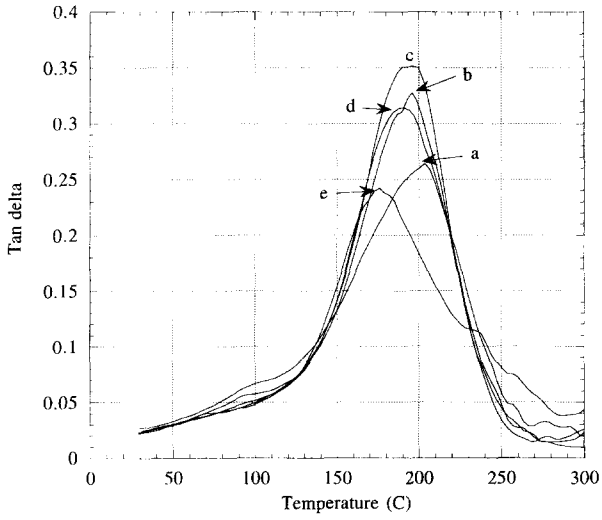

Figure 9 DMA curves as a function of temperature for N-butylmaleimide modified foams crosslinked with BMI-70: (a) Sample ButMI-7; (b) Sample ButMI-8; (c) Sample ButMI-9; (d) Sample ButMI-10; (e) Sample ButMI-11. All tan delta peaks occur at ≈ 199°C

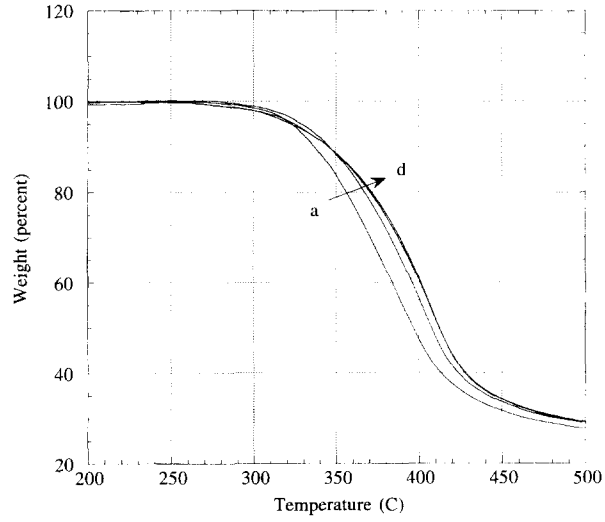

Figure 11 Thermogravimetric analysis in air of N-propylmaleimide modified foams crosslinked with BMI-70 showing increasing thermal stability with increasing propylmaleimide concentration from (a) Sample ProMI-7 to (d) Sample ProMI-10

trends as N-cyclohexylmaleimide with a peak in tan delta occurring at 219°C.

In the BMI-70 crosslinked N-propylmaleimide foams, similar behaviour is observed except the tan delta peak occurs at a lower temperature. *Figure 8* shows the DMA curves for the N-propylmaleimide foams with the same peak at 204°C. There does appear to be a slight decreasing trend in the temperature of the tan delta peak with increasing N-propylmaleimide concentration, but the most noticeable difference is the narrowing of the transition region.

Slightly different behaviour is observed with the BMI-70 crosslinked N-butylmaleimide foams. *Figure 9* shows the DMA curves for Samples ButMI-7 to ButMI-11. Although all samples tend to exhibit a tan delta peak at ≈ 199°C, at low N-butylmaleimide concentrations the DMA curves are skewed towards higher temperatures, and at high N-butylmaleimide concentrations the DMA curves are skewed towards lower temperatures. In addition, the DMA curves do not become narrower with increasing N-butylmaleimide concentration. The BMI-70 and the N-butylmaleimide appear to have a large difference in their individual T_g's, which produced a wide transition independent of concentration. In the DVB crosslinked N-butylmaleimide foams, a maximum peak of 160°C was obtained with 50% N-butylmaleimide by weight. In contrast, all other DVB crosslinked foams produced a T_g in excess of 200°C at high maleimide concentrations. Therefore, the large differences in thermal behaviour of the N-butylmaleimide and BMI-70 produce a polymeric foam with a wide T_g region.

Thermal stability

Thermal stability of the foam samples was evaluated in both air and nitrogen environments by thermogravimetric analysis. The three maleimides exhibited similiar behaviour for both the DVB and BMI crosslinked samples. *Figure 10* shows the TGA curves in air of the DVB crosslinked N-propylmaleimide foams. In sample ProMI-1, a two-step degradation process appears to be occurring for the 90%

styrene and 10% DVB foam system beginning at ≈ 275°C. With the addition of N-propylmaleimide, the degradation curves shift towards higher temperatures and the first degradation step decreases in size. When the same samples were tested in a nitrogen environment, a one-step degradation process was observed with the curves shifting towards higher thermal stability with increasing N-propylmaleimide concentration. The same behaviour was also observed in our previous work with N-ethylmaleimide.

As discussed in our work with N-ethylmaleimide, the first degradation step of the DVB crosslinked foams in air may be attributed to the degradation of the DVB crosslink. When BMI-70 crosslinked N-propylmaleimide foams were tested in air, a one-step degradation process beginning at ≈ 275°C was observed, shown in *Figure 11*. In addition, the TGA curve shifted towards high temperatures as the N-propylmaleimide concentration was increased. Therefore, it appears the increased thermal oxidative stability of the maleimide-styrene bond prevents the first degradation step and improves the overall thermal stability of the foam systems.

Mechanical performance

All samples were compression tested to evaluate the foam mechanical performance. Density and compression strengths of each of the foam samples are presented in *Table 4*, *Table 5* and *Table 6*. A corresponding specific compression strength (calculated by dividing the sample compression strengths by the sample densities) is included in the tables to allow a comparison of performance by accounting for density variations. All samples possessed specific compression strengths of 4.4–10.6 kPa cm^3/mg (10.2–24.7 psi ft^3/lb) except Samples ProMI-5, ProMI-6 and ButMI-6. However, a decreasing trend in compression strength was observed with increasing maleimide concentration for DVB crosslinked foams. BMI crosslinked foams showed a smaller decrease in compressive values as the total maleimide concentration (based on weight) increased.

Overall, the foam compression strength values corresponded to the quality of cell structure produced during processing. DVB crosslinked N-propylmaleimide and N-butylmaleimide foams had a large drop in compression strength when the concentration reached 40–50% by weight (Samples ProMI-5, ProMI-6 and ButMI-6). This drop in compression strength can be explained by the break down in cellular structure observed in the SEM photomicrographs at a 50% maleimide modifier concentration. In contrast, the N-cyclohexylmaleimide foams were able to retain higher compressive properties at high concentrations even though the foams contained solid polymer particles. These higher compression properties were due to the uniform open cell structure produced at all N-cyclohexylmaleimide concentrations.

CONCLUSIONS

This work has demonstrated that a wide range of N-substituted maleimides can be copolymerized with styrene

Table 4 Compression strengths of N-propylmaleimide modified foams

Sample	Density, mg/cm^3 (lb/ft^3)	Compression strength, kPa (psi)	Specific compression strength, kPa cm^3/mg (psi ft^3/lb)
ProMI-1	73.4 (4.58)	779 (113)	10.6 (24.7)
ProMI-2	72.9 (4.55)	724 (105)	9.93 (23.1)
ProMI-3	75.2 (4.69)	689 (100)	9.17 (21.3)
ProMI-4	78.7 (4.91)	517 (75.0)	6.57 (15.3)
ProMI-5	92.0 (5.74)	236 (34.3)	2.57 (6.0)
ProMI-6	97.3 (6.07)	61 (8.79)	0.63 (1.4)
ProMI-7	71.7 (4.48)	607 (88.0)	8.46 (19.7)
ProMI-8	69.5 (4.34)	609 (88.4)	8.77 (20.4)
ProMI-9	72.5 (4.53)	592 (85.9)	8.17 (19.0)
ProMI-10	74.5 (4.65)	483 (70.0)	6.48 (15.1)

Table 5 Compression strengths of N-butylmaleimide modified foams

Sample	Density, mg/cm^3 (lb/ft^3)	Compression strength, kPa (psi)	Specific compression strength, kPa cm^3/mg (psi ft^3/lb)
ButMI-1	73.4 (4.58)	779 (113)	10.6 (24.7)
ButMI-2	75.4 (4.71)	630 (91.4)	8.36 (19.4)
ButMI-3	80.2 (5.01)	663 (96.2)	8.27 (19.2)
ButMI-4	81.3 (5.08)	552 (80.1)	6.79 (15.8)
ButMI-5	85.8 (5.36)	378 (54.8)	4.40 (10.2)
ButMI-6	146 (9.11)	87 (12.6)	0.60 (1.4)
ButMI-7	69.3 (4.33)	593 (86.1)	8.56 (19.9)
ButMI-8	71.9 (4.49)	625 (90.7)	8.70 (20.2)
ButMI-9	70.0 (4.37)	560 (81.3)	8.01 (18.6)
ButMI-10	72.9 (4.55)	483 (70.0)	6.62 (15.4)
ButMI-11	75.6 (4.72)	367 (53.3)	4.86 (11.3)

Table 6 Compression strengths of N-cyclohexylmaleimide modified foams

Sample	Density, mg/cm^3 (lb/ft^3)	Compression strength, kPa (psi)	Specific compression strength, kPa cm^3/mg (psi ft^3/lb)
CyMI-1	73.4 (4.58)	779 (113)	10.6 (24.7)
CyMI-2	74.8 (4.67)	675 (97.9)	9.02 (21.0)
CyMI-3	78.4 (4.89)	672 (97.5)	8.57 (19.9)
CyMI-4	79.0 (4.93)	654 (94.9)	8.28 (19.2)
CyMI-5	82.1 (5.13)	620 (89.9)	7.55 (17.5)
CyMI-6	96.0 (5.99)	589 (85.4)	6.13 (14.2)
CyMI-7	68.1 (4.25)	462 (67.0)	6.78 (15.8)
CyMI-8	72.8 (4.54)	636 (92.2)	8.73 (20.3)
CyMI-9	72.5 (4.53)	624 (90.5)	8.60 (20.0)
CyMI-10	73.5 (4.59)	585 (84.8)	7.95 (18.5)

in a HIPE polymerization process to produce structural, polymeric foams with improved T_g's. The choice of N-substituted maleimide will dramatically affect the processing, thermal, and mechanical performance of each foam system. In terms of T_g improvements, a bulky or short chain N-substitution is preferred. N-cyclohexylmaleimide and N-ethylmaleimide provided approximately the same improvements in T_g. N-propylmaleimide produced a sacrifice in T_g performance, and N-butylmaleimide produced a severe sacrifice in T_g improvement.

In terms of processing performance, maleimide solubility in both water and styrene played important roles in the development of these foam systems. To incorporate high concentrations of maleimide modifiers, the N-substituted maleimide must possess a high solubility in styrene and a low solubility (preferably insolubility) in water. N-propylmaleimide and N-butylmaleimide allowed higher concentrations of maleimide modifiers to be incorporated into the foam systems because of their higher styrene solubility and lower water solubility in comparison to our previous work with N-ethylmaleimide. N-cyclohexylmaleimide demonstrated that solid polymer particles may appear throughout the foam structure once the styrene solubility is exceeded. Cyclohexylmaleimide also demonstrated the importance of using a water insoluble maleimide modifier.

The processing performance, T_g behaviour and thermal stability were greatly affected by the choice of crosslinker. When BMI-70 was substituted for DVB the emulsion viscosity increased significantly with increasing maleimide concentration. The substitution of BMI-70 for DVB also limited the relative amount of maleimide monomers that could be incorporated into the foams.

Finally, the maleimide modified foams produced structural properties with specific compression strengths of 4.4–10.6 kPa cm^3/mg. However, the foam compressive properties were dependent on the cellular morphology produced during processing. Lower compressive strengths were obtained when the cellular structure was disrupted.

ACKNOWLEDGEMENTS

The authors are grateful to Vivian Gurule for her efforts in taking the SEM pictures for this project. In addition, the authors would like to acknowledge the strong support of this work by Ainslie Young in the Department of Defense Program office at Los Alamos National Laboratory. This work was funded under contract W-7405-ENG-36 for the Department of Energy as part of the Laboratory Directed Research and Development program at Los Alamos National Laboratory.

REFERENCES

1. Barby, D. and Haq, A., European Patent No. 0,060,138, 1982.
2. Barby, D. and Haq, Z., European Patent No. 0,068,830, 1983.
3. Haq, Z., US Patent No. 4,536,521, 1985.
4. Barby, D. and Haq, Z., US Patent No. 4,522,953, 1985.
5. Jones, K., Lothian, B. R., Martin, A., Taylor, G. and Haq, Z., US Patent No. 4,611,014, 1986.
6. Jones, K., Lothian, B. R., Martin, A., Taylor, G. and Haq, Z., US Patent No. 4,612,334, 1986.
7. Jones, K., Lothian, B. R., Martin, A., Taylor, G. and Haq, Z., US Patent No. 4,668,709, 1987.
8. Edwards, C. J. C., Gregory, D. P. and Sharples, M., US Patent No. 4,788,225, 1988.
9. Bradley, G. M. and Stone, T. D., UK Patent No. 2,194,166, 1988.
10. Gregory, D. P., Sharples, M. and Tucker, I. M., European Patent No. 0,299,762, 1989.
11. Williams, J. M., Nyitray, A. M. and Wilkerson, M. H., US Patent No. 4,966,919, 1990.
12. Williams, J. M., Nyitray, A. M. and Wilkerson, M. H., US Patent No. 5,037,859, 1991.
13. Elmes, A. R., Hammond, K. and Sherrington, D. C., US Patent No. 4,985,468, 1991.
14. Sherrington, D. C. and Small, P. W., US Patent No. 4,965,289, 1990.
15. Hough, D. B., Hammond, K., Morris, C. and Hammond, R. C., US Patent No. 5,071,747, 1991.
16. Sherrington, D. C. and Small, P. W., US Patent No. 5,066,784, 1991.
17. Elmes, A. R., Hammond, K. and Sherrington, D. C., US Patent No. 5,021,462, 1991.
18. DesMarais, T. A., Dick, S. T. and Shiveley, T. M., US Patent No. 5,149,720, 1992.
19. DesMarais, T. A., Stone, K. J., Thompson, H. A., Young, G. A., LaVon, G. D. and Dyer, J. C., US Patent No. 5,260,345, 1993.
20. Beshouri, S. M., US Patent No. 5,200,433, 1993.
21. DesMarais, T. A., Dick, S. T. and Shiveley, T. M., US Patent No. 5,198,472, 1993.
22. Bass, R. M. and Brownscombe, T. F., US Patent No. 5,210,104, 1993.
23. DesMarais, T. A., Dick, S. T. and Shiveley, T. M., US Patent No. 5,250,576, 1993.
24. DesMarais, T. A., Stone, K. J., Thompson, H. A., Young, G. A., LaVon, G. D. and Dyer, J. C., US Patent No. 5,268,224, 1993.
25. DesMarais, T. A. and Stone, K. J., US Patent No. 5,292,777, 1994.
26. Brownscombe, T. F., Bass, R. M. and Corley, L. S., US Patent No. 5,290,820, 1994.
27. Bass, R. M. and Brownscombe, T. F., US Patent No. 5,306,734, 1994.
28. Williams, J. M., *Langmuir*, 1988, **4**, 44.
29. Williams, J. M. and Wrobleski, D. A., *Langmuir*, 1988, **4**, 656.
30. Williams, J. M., Gray, A. J. and Wilkerson, M. H., *Langmuir*, 1990, **6**, 437.

31. Williams, J. M., *Langmuir*, 1991, **7**, 1370.
32. Williams, J. M. and Wrobleski, D. A., *Journal of Materials Science Letters*, 1989, **24**, 4062.
33. Nyitray, A. M. and Williams, J. M., *Journal of Cellular Plastics*, 1989, **25**, 217.
34. Williams, J. M. and Wilkerson, M. H., *Polymer*, 1990, **31**, 2162.
35. Steckle, Jr., W.P., Duke, Jr., J.R. and Jorgensen, B.S., Cobalt dicarbollide containing polymer resins for cesium and strontium uptake, in *Metal Containing Polymeric Materials*, ed. C. U. Pittman *et al.* Plenum Publishing, New York, 1995.
36. Alexandratos, S. D., Beauvais, R., Duke, J. R. and Jorgensen, B. S., *Journal of Applied Polymer Science*, 1998, **68**, 1911.
37. Benicewicz, B. C., Jarvinen, G. D., Kathios, D. J. and Jorgensen, B. S., *Journal of Radioanalytical and Nuclear Chemistry*, submitted.
38. Hoisington, M. A., Duke, J. R. Jr. and Apen, P. G., *Polymer*, 1997, **38**(13), 3347.
39. Farbenindustrie, A. G., French Patent No. 844,554, 1939.
40. Alfrey, T. and Lavin, E., *Journal of the American Chemical Society*, 1945, **67**, 2044.
41. Coleman, L. E. Jr. and Conrady, J. A., *Journal Polymer Science*, 1959, **38**, 241.
42. Paesschen, G. V. and Timmerman, D., *Makromolekulare Chemie*, 1964, **78**, 112.
43. Cubbon, R. C. P., *Polymer*, 1965, **6**, 419.
44. Cubbon, T. C. P., *Journal of Polymer Science: Part C*, 1967, **16**, 387.
45. Barrales-Rienda, J. M., Gonzalez De La Campa, J. I. and Gonzalez Ramos, J., *Journal of Macromolecular Science and Chemistry*, 1977, **A11**(2), 267.
46. Mehta, N. B., Phillips, A. P., Lui, F. F. and Brooks, R. E., *Journal of Organic Chemistry*, 1960, **25**, 1012.